 CMES, vol.51, no.3, pp.191-212, 2009

An Efficient Petrov-Galerkin Chebyshev Spectral Method Coupled with the Taylor-series Expansion Method of Moments for Solving the Coherent Structures Effect on Particle Coagulation in the Exhaust Pipe

Chan T.L.[1,2], **Xie M.L.**[1,3] **and Cheung C.S.**[1]

Abstract: An efficient Petrov-Galerkin Chebyshev spectral method coupled with the Taylor-series expansion method of moments (TEMOM) was developed to simulate the effect of coherent structures on particle coagulation in the exhaust pipe. The Petrov-Galerkin Chebyshev spectral method was presented in detail focusing on the analyticity of solenoidal vector field used for the approximation of the flow. It satisfies the pole condition exactly at the origin, and can be used to expand the vector functions efficiently by using the solenoidal condition. This developed TEMOM method has no prior requirement for the particle size distribution (PSD). It is much simpler than the method of moment (MOM) and quadrature method of moments (QMOM), and is a promising method to approximate the aerosol general dynamics equation (GDE). The coupled fluid and particle fields were presented with three non-dimensional parameters (i.e., Reynolds number, Re; Schmidt number based on particle moment, Sc_M, and Damkohler number, Da in the governing equations). The temporal evolutions of the first three moments were discussed for different Damkohler numbers. The particle volume increases at all locations in the flow field, the larger the Damkohler number, the greater generation rate of large-scale particles. Far away from the eddy structure, the effect of the fluid convection on particle coagulation is small; however, the particle coagulation within the eddy core has an obvious wave-like distribution because of the large-scale eddy. The results reveal that the coherent structures play a significant role in the particle coagulation inside an exhaust pipe.

Keywords: exhaust pipe; nanoparticles; coagulation; moment method; spectral

[1] Research Centre for Combustion and Pollution Control, Department of Mechanical Engineering, The Hong Kong Polytechnic University, Kowloon, Hong Kong

[2] Corresponding author. Tel.: (852) 2766 6656; E-mail: mmtlchan@inet.polyu.edu.hk

[3] The State Key Laboratory of Coal Combustion, Huazhong University of Science and Technology, Wuhan, 430074, P.R. China

Galerkin method

1 Introduction

Nowadays, aerosol particles gradually become one of the most common unhealthy components of air pollution (Davidson *et al*. 2005; Sioutas *et al.*, 2005; Pope & Dockery 2006). Particle size and concentration affect not only the environment but also the health of human beings. Research have already shown that there is a strong correlation between mortality and particle size, with specific reference from nanoparticles (<50 nm or 0.05 μm) to fine particles (<2.5 μm) (Kittelson *et al*., 1998; Stone & Donaldson, 1998; Jacobson *et al.* 2005).

The evolution of nanoparticles is controlled by the general dynamic equation (GDE) which is a nonlinear partial differential equation (Friedlander, 2000). The GDE is capable of describing the particle evolution under all kinds of processes (i.e., convection, diffusion, coagulation, nucleation, surface growth and other physical or chemical phenomena, etc.). However, it is difficult to solve the GDE mainly because of its dependence on the particle volume. As a compromise, several scientific methods have been developed to cover this shortcoming. Among these scientific methods, the sectional method and nodal method (Prakash *et al.*, 2003; Miller *et al.*, 2004; Garrick *et al.*, 2006) divide the particle volume space into several discrete sections or bins. At each section or bin, the particle volume is considered as a constant and the GDE can be solved much more easily. Pohjola *et al.* (2003, 2006) utilized the sectional method to model the effect of the aerosol process for the dispersion of vehicular exhaust plumes in a street environment. Another kind of technique is the method of moment (MOM) (Pratsinis, 1988; Pratsinis & Kim, 1989; Settumba & Garrick, 2003; Chan *et al.*, 2006; Lin *et al.*, 2007). It takes the moments of the particle size distribution on the entire particle volume space. The GDE can be transformed into a set of moment equations. The closure problem arises when solving a finite number of moment equations which require the absent (usually a high order) moments to evaluate the correlative terms. Again some models will be introduced into the numerical simulation in order to solve the closure problem. The classical moment of method usually takes assumptions to make the moment equations closed, such as assuming that the particle size distribution is mono-dispersed or log-normal distributed. McGraw (1997) proposed a new method named the quadrature method of moment (QMOM) to make the moment equation closed. Based on the theory of McGraw (1997), Fox (2003) further developed a new method named the direct quadrature method of moment (DQMOM), which has proved to be compatible with QMOM in case of mono-variate functions. DQMOM also offers a powerful numerical approach for describing the poly-disperse solids which have undergone the segregation, growth, aggregation

and breakage processes in the context of computational fluid dynamics (CFD) simulations. So far as that is concerned, the QMOM and DQMOM are more suitable for engineering applications because of not only the accuracy but also the higher computational efficiency. For the QMOM, the major problem is that it needs to additionally solve an eigenvalue and eigenvector problem. For the DQMOM, it turns into solving a set of linear algebraic equations, and is more stable than the QMOM. Yu *et al.* (2008a) have recently presented a new numerical approach named the Taylor-series expansion method of moment (TEMOM) to solve the coagulation equation. In the TEMOM, the closure of the moment equations is approached using the Taylor-series expansion technique. Through constructing a system of the three first-order ordinary differential equations, the most important indexes for describing the aerosol dynamics, including the particle number density, particle mass and geometric standard deviation, are easily obtained. This approach has no prior requirement for the particle size spectrum, and the limitation existing in the log-normal distribution theory automatically disappears.

Several investigations on the nature of vehicular exhaust pollutants have been done. In the present study, the nanoparticle-laden flow in the vehicular exhaust tailpipe was investigated. There are two scientific problems to be solved namely the flow structure and particle evolution. Since the particles are too small (around nanometer magnitude), which means the Stokes number of particles $St \ll 1$ and so the particles follow the gas flow perfectly. It is reasonable to consider the flow and the particle fields separately and neglect the effect of particles on the gas flow (Xie *et al.*, 2007, 2008, 2009a, 2009b, 2009c).

In the present study, the particle behavior in the vehicular exhaust tailpipe where the nucleation and coagulation processes take place are the most important roles in the particle evolution. Nucleation of sulfuric acid is the major source of the vehicular exhaust plume, followed by the coagulation changes the exhaust particle size distributions. The nucleation is characterized by the parameterization for the sulfuric acid-water vapor (H_2SO_4-H_2O) binary system. For the coagulation, it is easy to write down the collision function for the free molecular regime and the continuum regime separately. It should be noted that the different regimes are denoted by the Knudsen number, Kn, while it is difficult to characterize the transition regime (Kn is intervenient between the free molecular regime and the continuum regime). Besides the simple interpolation suggested by Upadhyay & Ezekoye (2003), there is also an alternative treatment. Based on the flux-matching theory, the coagulation function is mainly expressed as an enhancement of the collision function for the near-continuum regime (Otto *et al.*, 1999). Once the collision function is determined, the coagulation effect can be calculated through the traditional collision theory.

As one of the generic flow features of fluid mechanics, the pipe flow has been the subject of scientific interest for over 125 years. An eminent scholar, Osborne Reynolds made the fundamental contribution to discover the key features of the transition to turbulence in the pipe flow: there is a lower critical Reynolds number below which no turbulence is observed; an upper critical one above which the laminar flow can no longer be sustained; and the minimal amplitude which perturbations have to exceed in order to cause the transition for intermediate Reynolds numbers. But the critical Reynolds number is difficult to define according to the description and interpretation of Mellibovsky & Meseguer (2009), and Echhardt (2009) due to the absence of a linear instability: an investigation of the Navier-Stokes equation can be rationally linearized around the parabolic velocity profile which shows that it is linearly stable for all Reynolds numbers (Meseguer & Trefethen, 2003). The nonlinearity is essential for turbulent flow. But with the inclusions of nonlinear items, other persistent flow structures around which the turbulent flow organizes itself can exist, very much as in other systems where the periodic orbits carry chaotic dynamics (Echhardt, 2009; Hof *et al*., 2004 & 2006; Pringle & Kerswell, 2004; Eckhardt, 2008). The studies of Trefethen *et al.* (1993) highlighted the fact that even when all eigenvalues of the linearized problem indicate the decay, there can be transient amplification and growth in energy owing to the non-normality of the linearized operator. The efficiency of the Petrov-Galerkin spectral method was discussed by Meseguer & Trefethen (2003) and Lin & Atluri (2000, 2001), and the eigenvalues were numerically computed based on the Chebyshev polynomial spectral method. Recently, Bierbrauer & Zhu (2007) have presented that the three analytical solutions, the bounded creeping flow, solenoidal and conserved solenoidal solutions, which are both continuous, incompressible, retain as much of the original mathematical formulation as possible and provide a physically reasonable initial velocity field. Mohammadi (2008) and Orsini *et al.* (2008) have proposed a meshless radial basis function technique while Sellountos & Sequeira (2008, 2009) have applied the radial basis function networks for the computation of transient viscous flows. Liu & Atluri (2008 & 2009) have developed a highly accurate technique based on the modified Trefftz method to deal with the ill-posed linear problems. A link between these transition flow structures has recently been discussed by van Doorne & Westerweel (2009). Theoretical approaches to extract the perturbations that are efficient in triggering turbulence have been presented by Biau & Bottaro (2009), and Cohen *et al.* (2009), respectively. Xie *et al.* (2009d, 2009e) have expanded the Petrov-Galerkin Chebyshev spectral method coupled with the exponential coordinate transformation to the linear stability analysis of circular jet flow. The numerical results have agreement with our previous results of Chan *et al*. (2008).

The coherent structures of the flow play a fundamental role in the transition to

turbulence and the formation of coherent vortex structures in a turbulent fluid. It turns out that all these coherent structures are unstable and can appear transiently in the dynamic system. Nevertheless, they can be identified in the experimental and numerical simulations (Hof *et al.*, 2004; Kerswell & Tutty, 2007; Schneider *et al.*, 2007; Duggleby *et al.*, 2009). Some of these flow structures might be related to the coherent traveling waves. For instance, the proper orthogonal decomposition provides the first evidence for the helical traveling waves which also exists as the exact coherent structures (Duguet *et al.*, 2008).

The aim of this paper is intended to simulate the three-dimensional flow structures and particle evolution in the vehicular exhaust pipe. An improved Petrov-Galerkin Chebyshev spectral method coupled with the Taylor-series expansion method of moments (TEMOM) will be developed to simulate the effect of coherent structures on the particle coagulation in the exhaust pipe.

2 The mathematical formulation

2.1 Flow fields

The flow is considered to be the constant density shear flow containing the nano-scale particles. The primary transport variables for the flow field are the fluid velocity and pressure. These variables are governed by the Navier-Stokes equations:

$$\frac{\partial u_j}{\partial x_j} = 0 \tag{1}$$

$$\frac{\partial u_i}{\partial t} + \frac{\partial u_i u_j}{\partial x_j} = -\frac{1}{\rho}\frac{\partial p}{\partial x_i} + \nu \frac{\partial^2 u_j}{\partial x_j \partial x_j} \tag{2}$$

where ρ is the fluid density; ν is the kinetic viscosity; u_i is the velocity component in the coordinate x_i direction.

2.2 Particle fields

The transport of the nano-scale particles dispersed through the fluid is governed by the aerosol general dynamics equations (GDE). The GDE describes the particle dynamics under the effect of different physical and chemical processes: convection, diffusion, coagulation, surface growth, nucleation and the other internal/external forces (Friedlander, 2000). In the present study, the Brownian coagulation in the

free molecule regime is solely considered, and the GDE can be written as:

$$\frac{\partial n}{\partial t}+\frac{\partial u_j n}{\partial x_j}=\frac{\partial}{\partial x_j}\left(D_n\frac{\partial n}{\partial x_j}\right)+\frac{1}{2}\int_0^v \beta(v,v-v_1)n(v_1,t)n(v-v_1,t)dv_1 - \int_0^v \beta(v_1,v)n(v,t)n(v_1,t)dv_1 \quad (3)$$

where $n(v,t)$ is the number of particles of volume v at time t; β is the collision frequency function for coagulation in free molecule regime, which is given by:

$$\beta = B_1\left(1/v+1/v_1\right)^{1/2}\left(v^{1/3}+v_1^{1/3}\right)^2 \quad (4)$$

where the collision factor constant $B_1 = (3/4\pi)^{1/6}(6K_bT/\rho)^{1/2}$; K_b is the Boltzmann's constant. D_n is the diffusion coefficient in the free molecule regime, which is given by:

$$D_n = \frac{(3/4\pi)^{1/3}K_bT}{v^{2/3}\rho c(1+\pi\alpha/8)} \quad (5)$$

where c is the mean thermal speed; α is the accommodation coefficient; T is the fluid temperature. From a practical point of view (Garrick *et al.*, 2006; Settumba & Garrick, 2003), the GDE is computationally unfeasible to solve directly except for the small range of discrete particle sizes. In order to overcome this problem, a moment method is utilized to describe the particle field in time and space. The $k-$th order moment M_k of the particle distribution is defined as:

$$M_k = \int_0^\infty v^k n(v)dv \quad (6)$$

A transport equation for M_k is obtained by multiplying both sides of the GDE with v^k and integrating over all particle sizes (Pratsinis, 1988). The transport equation for the $k-$th order moment M_k is expressed as:

$$\frac{\partial M_k}{\partial t}+\frac{\partial u_j M_k}{\partial x_j}=\frac{\partial}{\partial x_j}\left(\kappa\frac{\partial M_{k-2/3}}{\partial x_j}\right)+\left[\frac{dM_k}{dt}\right]_{coag} \quad (7)$$

where the size-independent diffusivity is $\kappa = D_n \times v^{2/3}$; $[dM_k/dt]_{coag}$ is the source term due to the Brownian coagulation and can be expressed by Upadhyay and Ezekoye (2003):

$$\left[\frac{dM_k}{dt}\right]_{coag}=\frac{1}{2}\int_0^\infty\int_0^\infty\left[\left(v+v_1\right)^k-v^k-v_1^k\right]\beta(v,v_1)n(v,t)n(v_1,t)\,dv\,dv_1 \quad (8)$$

where k= 0, 1, 2,....

The minimum number of moments required is the first three, M_0, M_1 and M_2. The zeroth moment M_0 is the total particle number concentration; the first moment M_1 is proportional to the total particle mass; the second moment M_2 is proportional to the total light scattered (Friedlander, 2000). According to the prior developed Taylor-series expansion method of moment (TEMOM) (Yu *et al.*, 2008a, 2008b & 2008c), the source term in the first three moments can be written as:

$$\left[\frac{dM_0}{dt}\right]_{coag} = \frac{\sqrt{2}B_1\left(65M_C^2 - 1210M_C - 9223\right)M_0^2}{5184\left(M_0/M_1\right)^{1/6}} \tag{9}$$

$$\left[\frac{dM_0}{dt}\right]_{coag} = 0 \tag{10}$$

$$\left[\frac{dM_2}{dt}\right]_{coag} = -\frac{\sqrt{2}B_1\left(701M_C^2 - 4210M_C - 6859\right)M_1^2}{2592\left(M_0/M_1\right)^{1/6}} \tag{11}$$

where the dimensionless moment M_C is defined as:

$$M_C = \frac{M_2 M_0}{M_1^2} \tag{12}$$

In order to obtain the fractional moments in equation (7), a Taylor-series expansion technique is used to close the moment equations. In equation (8), v^k can be expanded with Taylor-series about the point $v = V$, and $V(=M_1/M_0)$ is the mean particle size which is consistent with the expansion point proposed by Yu *et al.* (2008a; 2008b and 2008c).

$$v^k = V^k + ku^{k-1}(v-V) + \frac{k(k-1)V^{k-2}}{2}(v-V)^2 + \cdots \tag{13}$$

Similar to the disposition by Yu *et al.* (2008a, 2008b and 2008c), the first three terms of the Taylor-series are taken in order to meet the requirement of moment transformation. Hence, it is necessary to group the truncated terms in equation (13) as:

$$v^k = \frac{k(k-1)V^{k-2}}{2}v^2 - k(k-2)V^{k-1}v + \frac{(k-1)(k-2)}{2}V^k \tag{14}$$

Substituting equation (14) into equation (8),

$$M_k = \int_0^\infty v^k n(v)dv = \frac{k(k-1)V^{k-2}}{2}M_2 - k(k-2)V^{k-1}M_1 + \frac{(k-1)(k-2)V^k}{2}M_0$$

(15)

Then the three fractional moments $M_{-2/3}$, $M_{1/3}$ and $M_{4/3}$ that appeared in the first three moment equations can be expressed as:

$$M_{-2/3} = \frac{(4+5M_C)M_0}{9V^{2/3}};\ M_{1/3} = \frac{(10-M_C)M_1}{9V^{2/3}};\ M_{4/3} = \frac{(7+2M_C)M_2}{9V^{2/3}M_C} \tag{16}$$

Then equation (7) can be expressed explicitly as:

$$\frac{\partial M_0}{\partial t} + \frac{\partial u_j M_0}{\partial x_j} = \kappa \frac{\partial}{\partial x_j}\left(\frac{\partial}{\partial x_j}\frac{(4+5M_C)M_0}{9V^{2/3}}\right) + \frac{\sqrt{2}B_1\left(65M_C^2 - 1210M_C - 9223\right)M_0^2 V^{1/6}}{5184} \tag{17}$$

$$\frac{\partial M_1}{\partial t} + \frac{\partial u_j M_1}{\partial x_j} = \kappa \frac{\partial}{\partial x_j}\left(\frac{\partial}{\partial x_j}\frac{(10-M_C)M_1}{9V^{2/3}}\right) \tag{18}$$

$$\frac{\partial M_2}{\partial t} + \frac{\partial u_j M_2}{\partial x_j} = \kappa \frac{\partial}{\partial x_j}\left(\frac{\partial}{\partial u_j}\frac{(7+2M_C)M_2}{9V^{2/3}M_C}\right) - \frac{\sqrt{2}B_1\left(701M_C^2 - 4210M_C - 6859\right)M_1^2 V^{1/6}}{2592} \tag{19}$$

It is obvious that equations (17–19) is the system of partial differential equations and all terms are denoted by the first three moments M_0, M_1 and M_2, and thus the system can be automatically closed. Under these conditions, the first three moments for describing aerosol dynamics are obtained through solving the systems of partial differential equations. Here, the whole derivation of equations (17–19) for the particle fields does not involve any assumptions for the particle size distribution (PSD), and the final mathematical form is much simpler than the method of moment (MOM) (Garrick *et al*., 2006; Pratsinis, 1988; Settumba & Garrick, 2003; Yu *et al*., 2008a; 2008b and 2008c).

2.3 Non-dimensionalization

The governing equations are non-dimensionalized to simplify the treatment and analysis of the interactions between the hydrodynamic and particle fields. They can be accomplished using the following relations:

$$t^* = \frac{t}{R/U_\tau};\ r^* = \frac{r}{R};\ z^* = \frac{z}{R};\ u_i^* = \frac{U_\tau}{u_i};\ p^* = \frac{p}{\rho U_\tau^2};\ M_k^* = \frac{M_k}{M_{k0}} \tag{20}$$

The characteristic length R is the radius of the pipe; the characteristic velocity $U_\tau = (\tau_w/\rho)^{1/2}$ is the shear velocity based upon the wall shear stress τ_w; ρ is the fluid density; M_{k0} is the reference value of the k-th moment. Substituting the relations given in equation (20) into equations (1) and (2) yields the familiar mass and momentum conservation equations in terms of cylindrical coordinates (the star symbol '$*$' is ignored thereafter):

$$\frac{\partial u_r}{\partial r} + \frac{u_r}{r} + \frac{1}{r}\frac{\partial u_\theta}{\partial \theta} + \frac{\partial u_z}{\partial z} = 0 \tag{21}$$

$$\frac{Du_r}{Dt} - \frac{u_\theta^2}{r} = -\frac{\partial p}{\partial r} + \frac{1}{Re}\left(\Delta u_r - \frac{u_r}{r^2} - \frac{2}{r^2}\frac{\partial u_\theta}{\partial \theta}\right) \tag{22}$$

$$\frac{Du_\theta}{Dt} + \frac{u_r u_\theta}{r} = -\frac{1}{r}\frac{\partial p}{\partial \theta} + \frac{1}{Re}\left(\Delta u_\theta - \frac{u_\theta}{r^2} + \frac{2}{r^2}\frac{\partial u_r}{\partial \theta}\right) \tag{23}$$

$$\frac{Du_z}{Dt} = -\frac{\partial p}{\partial z} + \frac{1}{Re}\Delta u_z \tag{24}$$

where the operators $\Delta \equiv \frac{\partial^2}{\partial r^2} + \frac{1}{r}\frac{\partial}{\partial r} + \frac{1}{r^2}\frac{\partial^2}{\partial \theta^2} + \frac{\partial^2}{\partial z^2}$; $\frac{D}{Dt} \equiv \frac{\partial}{\partial t} + u_r\frac{\partial}{\partial r} + \frac{u_\theta}{r}\frac{\partial}{\partial \theta} + u_z\frac{\partial}{\partial z}$, and Reynolds number $Re = U_\tau R/\nu$.

Similarly, for the particle field, the non-dimensionalized equations for the first three moment equations are given by:

$$\frac{DM_0}{Dt} = \frac{1}{Sc_M Re}\Delta\frac{(4+5C_M M_C)M_0}{9V^{2/3}} + Da\frac{\left(65C_M^2M_C^2 - 1210C_M M_C - 9223\right)M_0^2 V^{1/6}}{5184} \tag{25}$$

$$\frac{DM_1}{Dt} = \frac{1}{Sc_M Re}\Delta\frac{(10-C_M M_C)M_1}{9V^{2/3}} \tag{26}$$

$$\frac{DM_2}{Dt} = \frac{1}{Sc_M Re}\Delta\frac{(7+2C_M M_C)M_2}{9C_M M_C V^{2/3}} - Da\frac{\left(701C_M^2M_C^2 - 4210C_M M_C - 6859\right)M_1^2 V^{1/6}}{2592C_M} \tag{27}$$

where the Schmidt number based on the particle moment, Sc_M is:

$$Sc_M = \nu/(\kappa/V_0^{2/3}) \tag{28}$$

The initial mean particle volume V_0 is determined by the reference moment M_{k0} (i.e., $V_0 = M_{10}/M_{00}$) and $C_M = M_{20} \times M_{00}/M_{10}^2$ is a constant. It should be noted that C_M is the polydispersity index and is unity in monodisperse aerosol (Pratsinis,

1988). The Damkohler number, *Da*, represents the ratio of the convective time scale to the coagulation time scale and is given by:

$$Da = \frac{\sqrt{2}B_1 M_{00} V_0^{1/6}}{U_\tau / R} = \frac{\sqrt{2}B_1 C}{U_\tau \Big/ R V_0^{5/6}} \tag{29}$$

where C is the initial volume fraction $C = M_{00}V_0/M_{10}$ and is defined as the ratio of the volume of the particles to the volume of the fluid. In the pipe flow under consideration, the characteristic length and velocity scales, as well as the volume fraction, are the primary means of controlling the rate of coagulation. Any changes of these quantities have the effect of increasing or decreasing the Damkohler numbers. This non-dimensional number therefore serves as a single parameter to characterize the coagulation growth in hydrodynamic flow. Damkohler numbers of zero and infinity represent the limiting flow conditions, where zero indicates that the particles do not collide while infinity implies that collisions occur instantaneously, and all particles are instantaneously converted to the largest particle (Garrick *et al*., 2006; Settumba & Garrick, 2003).

2.4 The linear stability and coherent structures in the exhaust pipe

For the numerical solution of the Navier-Stokes equations, the dependent variables for the perturbation of the velocity field from the laminar solution can be taken as:

$$u_r = U_r + u_r'; u_\theta = U_\theta + u_\theta'; u_z = U_z + u_z'; p = P + p' \tag{30}$$

where the velocity components are interacted linearly and nonlinearly. In the present study, it is a linearized problem in which only the infinitesimal perturbations from the laminar flow are considered. It can be achieved by setting the quadratic terms with respect to such perturbations to zero. The solutions of these equations can be expressed as the super-positions of complex Fourier modes:

$$\frac{u_r'}{u_r(r)} = \frac{u_\theta'}{u_\theta(r)} = \frac{u_z'}{u_z(r)} = \frac{p'}{\rho p(r)} = e^{i(n\theta + kz - \beta t)} = e^{i(n\theta + kz - kct)} \tag{31}$$

The linearized Navier-Stokes equations can be written as:

$$-ikcu_r = -Dp + \frac{1}{Re}\left(D^2 u_r + \frac{1}{r}u_r - \frac{n^2+1}{r^2}u_r - k^2 u_r - \frac{2}{r^2}inu_\theta\right) - ikU_z u_r \tag{32}$$

$$-ikcu_\theta = -\frac{in}{r}p + \frac{1}{Re}\left(D^2 u_\theta + \frac{1}{r}u_\theta - \frac{n^2+1}{r^2}u_\theta - k^2 u_\theta + \frac{2}{r^2}inu_r\right) - ikU_z u_\theta \tag{33}$$

$$-ikcu_z = -ikp + \frac{1}{Re}\left(D^2u_z + \frac{1}{r}u_z - \frac{n^2}{r^2}u_z - k^2u_z\right) - u_rDU_z - ikU_zu_z \tag{34}$$

$$\left(D + \frac{1}{r}\right)u_r + i\left(\frac{1}{r}nu_\theta + ku_z\right) = 0 \tag{35}$$

The corresponding boundary conditions are:

$$u_r(1) = u_\theta(1) = u_z(1) = 0 \tag{36}$$

The solenoidal vector field can be expressed as:

$$\mathbf{u} = e^{i(kz+n\theta-kct)}\sum_{m=0}^{M} a_m^{(1)}\mathbf{w}_m^{(1)}(r)\mathbf{u}_m^{(1)}(r) + a_m^{(2)}\mathbf{w}_m^{(2)}(r)\mathbf{u}_m^{(2)}(r) \tag{37}$$

For case n = 0: The suitable basis functions which satisfied the solenoidal conditions can be written as:

$$\mathbf{u}_m^{(1)}(r) = \left(\begin{bmatrix}0\\ rh_m(r)\\ 0\end{bmatrix}\right)\mathbf{u}_m^{(2)}(x) = \left(\begin{bmatrix}-ikrg_m(r)\\ 0\\ D_+[rg_m(r)]\end{bmatrix}\right) \tag{38}$$

where m = 0, 1,... except if k = 0, the third component of $\mathbf{u}_m^{(2)}$ is replaced by $h_m(r)$ where $h_m(r)$ = (1-r^2)$T_{2m}(r)$, and $g_m(r)$ = (1-r^2)$^2T_{2m}(r)$, and $T_{2m}(r)$ are the Chebyshev polynomial of degree $2m$. So much for the bases for the functions **u**, the functions **w** can also be taken as the same bases. However, the resulting matrices would be dense, whereas they can be made to be banded as follows:

$$\tilde{\mathbf{w}}_m^{(1)}(r) = \frac{1}{\sqrt{1-r^2}}\begin{pmatrix}0\\ h_m(r)\\ 0\end{pmatrix} \tag{39}$$

$$\tilde{\mathbf{w}}_m^{(2)}(r) = \frac{1}{\sqrt{1-r^2}}\begin{pmatrix}ikr^2g_m(r)\\ 0\\ D_+[r^2g_m(r)] + r^3h_m(r)\end{pmatrix} \tag{40}$$

where '$\sim$' represents the complex conjugate, m = 0, 1,.. except if k = 0, and the third component of $\mathbf{w}_m^{(2)}$ is replaced by $rh_m(r)$.

For case n $\neq$ 0: The similar physical (or trial) basis and the dual (or test) basis can be obtained accordingly (Meseguer & Trefethen, 2003).

2.5 The initial conditions for particles

The initial particle distribution of the present study is assumed to be the log-normal distribution; and the size distribution function is defined by Lee (1983) and Pratsinis (1988):

$$n(v,t) = \frac{N}{3\sqrt{2\pi}v\ln\sigma}\exp\left(-\frac{\ln^2(v/v_g)}{18\ln^2\sigma}\right) \tag{41}$$

The geometric mean volume and standard deviation are expressed as the functions of the first three moments:

$$v_g = \frac{M_1^2}{M_0^{3/2}M_2^{1/2}}; \quad \ln^2\sigma = \frac{1}{9}\ln\left(\frac{M_2M_0}{M_1^2}\right) \tag{42}$$

The initial k-th moments M_{k0} are expressed as:

$$M_{k0} = Nv_g^k\exp\left(9k^2\ln^2\sigma/2\right) \tag{43}$$

It should be noted that different researchers use different forms for the width parameter of standard deviation in the log-normal distribution (e.g., Barrett & Jheeta (1996) used w_g= lnσ /3). Under the case of the initial log-normal distribution with N= 1, v_g= $3^{1/2}$/2 and lnσ= $(\ln 4/3)^{1/2}$/3 which is consistent with the initial condition used by Barrett & Jheeta (1996), then the initial k-th moments for k= 0, 1, 2 are M_{00}= 1, M_{10}= 1 and M_{20}= 4/3, respectively.

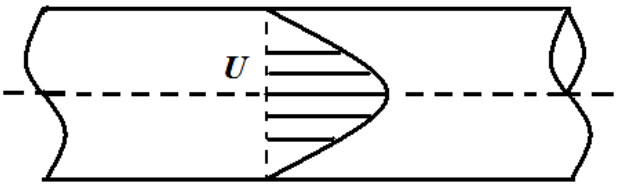

Figure 1: Configuration of a circular pipe flow.

3 Results and discussion

3.1 Flow configuration

The flow under consideration is a three dimensional, incompressible pipe flow, and the flow configuration is shown in Figure 1. The Reynolds number at the flow

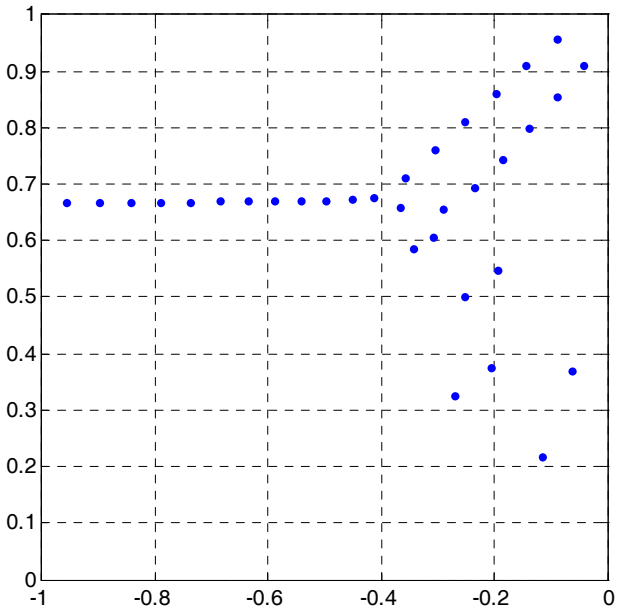

Figure 2: Calculated eigenvalues in the complex plane for $n = 1$ and $k = 1$ with $Re_m = 3000$.

is about 55. When it is non-dimensionalized with the maximum velocity U_m, the Reynolds number is $Re_m = 3000$. The formation of large scale structures is expedited through the addition of an eigenfunction based on the perturbation to the velocity field. In the present study, the azimuthal mode of the disturbance, $n = 1$ and the axial wavenumber of the perturbation, $k = 1$. The calculated eigenvalues are shown in Figure 2 based on the numerical algorithm proposed by Meseguer and Trefethen (2003). The corresponding perturbation stream functions are shown in Figure 3. The fluid in the present study is air at 300 K. Initially, the stream is seeded with particles of mean diameter 1 nm. At this condition, the Schmidt number is $Sc_M = 3$. Three different Damkohler number flows suggested by Settumba & Garrick (2003) and Garrick *et al.* (2006) were simulated to be 0.2, 1.0 and 2.0.

3.2 Numerical method

Computation was performed on a domain of 2π in the streamwise direction with a unit disk in the transverse profile, the coupled nonlinear items in the different moment equations are solved using the four-order Runge-Kutta method. A significant portion of numerical simulation used the spectral Galerkin method, which is an

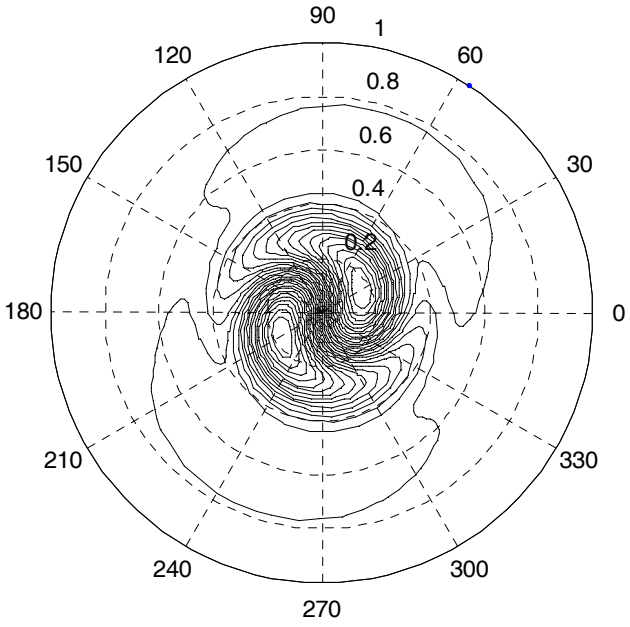

Figure 3: The perturbation stream functions of the center mode for the rightmost eigenvalues.

efficient and accurate numerical scheme for the axisymmetric Navier-Stokes equations in the primitive variables in a circular pipe. The scheme presented by Lopez & Shen (1998) was based on a spectral Galerkin approximation for the space variables and a second-order projection scheme for the time variable. To avoid the singularity in cylindrical coordinates and time step restriction, a Fourier filter in the azimuthal direction was used. The Chebyshev expansion in the radial direction on [-1, 1] over the coordinate singularity was used instead of [0, 1] (Fornberg & Sloan, 1994; Fornberg, 1995). Furthermore, Xie *et al*. (2009d) have recently used an improved Petrov-Galerkin spectral collocation solution for the linear stability of circular jet.

3.3 Evolution of the moments

The changes of different particle moments along the radial direction are shown in Figure 4. As the particles collide and coagulate, the particle number concentration decreases. This is revealed in the 0-th particle moment, M_0. As time progresses, the decreasing ratio of M_0 is different. Outside the large-scale motion of the eddy at the axial domain, the behavior of the coagulation is similar to that for the zero-

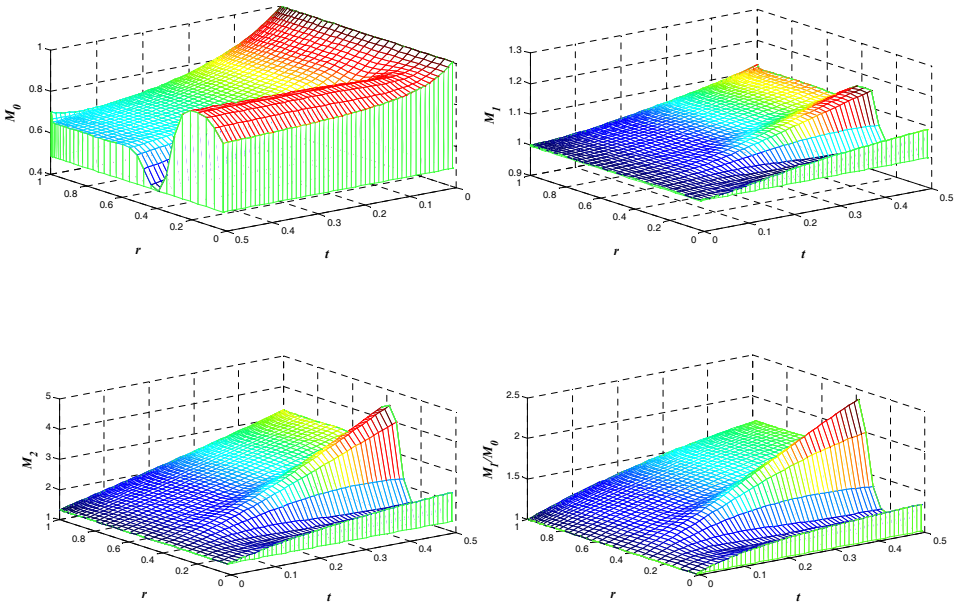

Figure 4: Evolution of the particle moments at different points along the radial direction.

dimensional case. The effect of convection or the flow coherent structure is small. However, the role of the convection in the large-scale motion is significant, and the distribution of the moments is similar to that of the perturbation velocity stream function along the radius of a circular exhaust pipe as shown in Figure 3. The effect of the convection can also be found in Figures 5 and 6. In an initially monodisperse aerosol, the coagulation creates new particles of different sizes. This alters the second moment. Generally the second moment increases throughout the flow field. However, the changes along the radial direction are different, which is similar with the changes of the zero-order particle moment, but the locations of their maximum and minimum values are contrary to those of the zero-order particle moment. The growth of particle size may be quantified by the mean particle volume V which is calculated from the ratio of the first two moments $V = M_1/M_0$. The evolution and distribution of the mean particle volume is similar to that of the second particle moment.

3.4 Effect of Damkohler number

The particle coagulation Damkohler number, Da, is defined to represent the ratio of convection to coagulation time scales in the different moment equations (Settumba

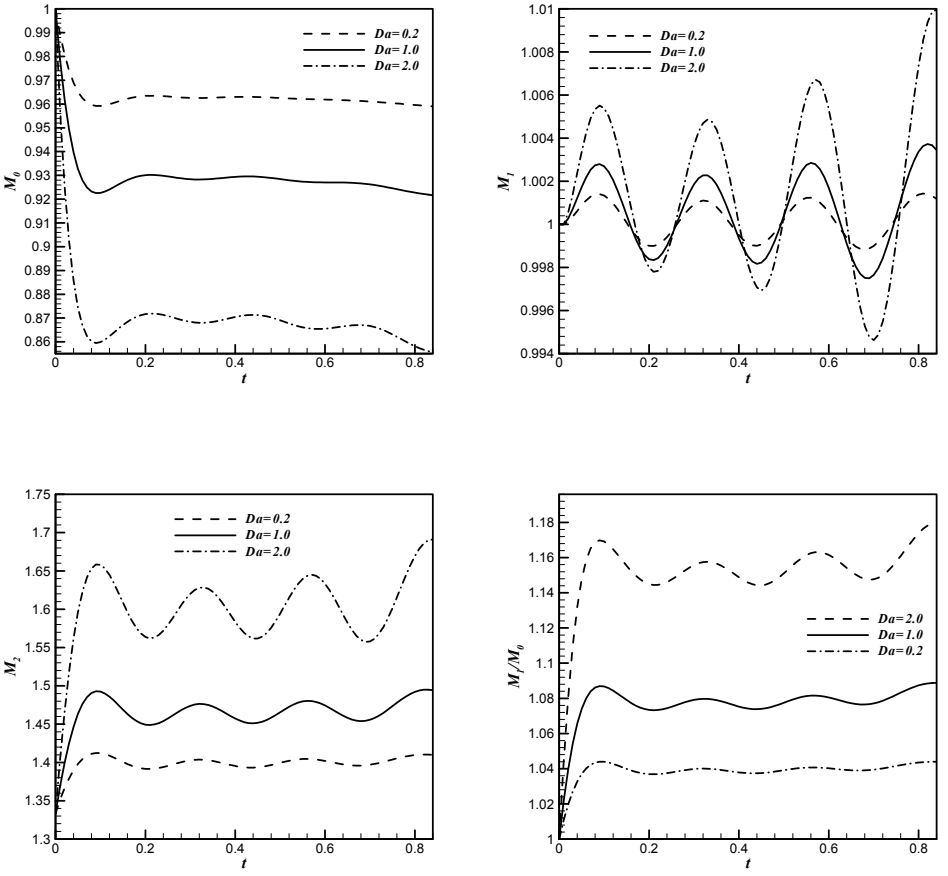

Figure 5: Evolution of the particle moments in the vortex core.

and Garrick, 2003). The larger the Damkohler number, the smaller characteristic coagulation time scale, and the greater generation rate of large-scale particles. The effects of the Damkohler number are shown in Figures 5 and 6 for different locations along the radial direction. For a certain moment Schmidt number (i.e., Sc_M= 3), the evolutions of the particle zero and second order moments have three different levels which are the representation of the characteristic coagulation time scales. The particle evolution of the first order moment in the vortex core fluctuates near the mean values as shown in Figure 5. The fluctuation frequency is proportional to the product of the radius in situ and inverse of the perturbation velocity.

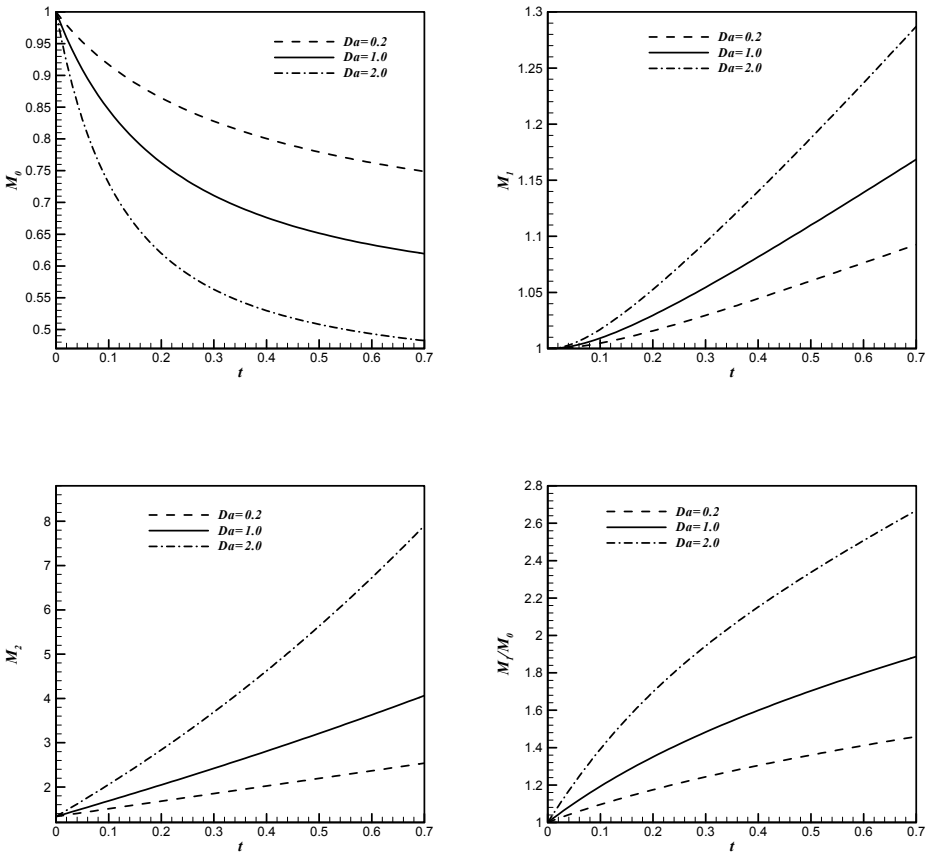

Figure 6: Evolution of the particle moments near the circular pipe wall.

4 Conclusion

Numerical simulation of particle coagulation in the exhaust pipe was performed. The flow field was obtained by solving the incompressible Navier-Stokes equations. The formation of large-scale structures was expedited through the addition of an eigenfunction based on the perturbation to the velocity field. The Taylor series expansion method of moments (TEMOM) was used to approximate the particle general dynamic equations (GDE).

The coupled fluid and particle fields were presented with three non-dimensional parameters (i.e., Reynolds number, Re; Schmidt number based on particle moment, Sc_M, and Damkohler number, Da in the governing equations. Three typical Damkohler numbers were performed covering one order of magnitude while the

Reynolds number and moment Schmidt number were kept constant.

The particle volume increases at all locations in the flow field, the larger the *Da*, the greater the generation rate of large-scale particles. Far away from the eddy structure, the effect of the fluid convection on particle coagulation is small; however, the particle coagulation within the eddy core has an obvious wave-like distribution because of the large-scale eddy. The results reveal that the coherent structures play a significant role in the particle coagulation inside an exhaust pipe.

Acknowledgement: This work was supported by grants from the Departmental and Central Research Grants of The Hong Kong Polytechnic University (Project Nos. G-YG83 and G-YH83). The second author would also like to acknowledge the support of the National Natural Science Foundation of China with Grant No. 50806023.

References

Barrret, J. C.; Jheeta, S. J. (1996): Improving the accuracy of the moments method for solving the aerosol general dynamic equation. *J. Aerosol Sci.*, vol. 27, pp.1135-1142.

Biau, D.; Bottaro, A. (2009): An optimal path to transition in a duct. *Philos. Trans. R. Soc. A- Math. Phys. Eng. Sci.*, vol. 367, pp. 529-544.

Bierbrauer, F.; Zhu, S. P. (2007): A solenoidal initial condition for the numerical solution of the Navier-Stokes equations for two-phase incompressible flow. *CMES: Computer Modeling in Engineering & Sciences*, vol. 19, pp. 1-22.

Chan, T. L.; Lin, J. Z.; Zhou, K.; Chan, C. K. (2006): Simultaneous numerical simulation of nano and fine particle coagulation and dispersion in a round jet. *J. Aerosol Sci.*, vol. 37, pp. 1545-1561.

Cohen, J.; Philip, J.; Ben-Dov, G. (2009): Aspects of linear and nonlinear instabilities leading to transition in pipe and channel flows, *Philos. Trans. R. Soc. A-Math. Phys. Eng. Sci.*, vol. 367, pp. 509-527.

Davidson, C. I.; Phalen, R. F., Solomon, P. A. (2005): Airborne particulate matter and human health: A review. *Aerosol Sci. Technol.*, vol. 39, pp. 737-749.

Duggleby, A. K.; Kenneth, B.; Schwaenen, M. (2009): Structure and dynamics of low Reynolds number turbulent pipe flow. *Philos. Trans. R. Soc. A- Math. Phys. Eng. Sci.*, vol. 367, pp. 473-488.

Duguet, Y.; Willis, A. P.; Kerswell, R. R. (2008): Transition in pipe flow: the saddle structure on the boundary of turbulence. *J. Fluid Mech*. vol. 613, pp. 255-274.

Eckhardt, B. (2008): Turbulence transition in pipe flow: some open questions. *Nonlinearity*, vol. 21, pp. 1-11.

Eckhardt, B. (2009): Introduction. Turbulence transition in pipe flow: 125th anniversary of the publication of Reynolds' paper. *Philos. Trans. R. Soc. A- Math. Phys. Eng. Sci.*, vol. 367, pp. 449-455.

Fornberg, B.; Sloan, D. M. (1994): A review of pseudospectral methods for solving partial differential equation, *Acta Numerica*, vol. 3: 203–267.

Fornberg, B. (1995): A pseudospectral approach for polar and spherical geometries. *SIAM J. Sci. Comput.*, vol.16, pp. 1071-1081.

Friedlander, S. K. (2000): Smoke, Dust, and Haze: Fundamentals of Aerosol Dynamics, Oxford University Press, 2nd edition.

Fox R. O. (2003): Computational Models for Turbulent Reacting Flows, Cambridge University Press.

Garrick, S. C.; Lehtinen, K. E. J.; Zachariah, M. R. (2006): Nanoparticle coagulation via a Navier Stokes nodal methodology: Evolution of the particle field. *J. Aerosol Sci.,* vol. 37, pp. 555-576.

Hof, B.; van Doorne, C. W. H.; Westerveel, J.; Nieuwstadt, F. T. M.; Faisst, H.; Eckhardt, B.; Wedin, H.; Kerswell, R. R.; Waleffe, F. (2004): Experimental observation of nonlinear travelling waves in turbulent pipe flow. *Science*, vol. 305, pp. 1594-1598.

Hof, B.; Westerweel, J.; Schneider, T. M.; Eckhardt, B. (2006): Finite lifetime of turbulence in shear flows. *Nature*, vol. 443, pp. 59-62.

Jacobson, M. Z.; Kittelson, D. B.; Watts W. F. (2005): Enhanced coagulation due to evaporation and its effect on nanoparticle evolution. *Environ. Sci. Tech.*, vol. 39, pp. 9486-9492.

Kerswell, R. R.; Tutty, O. R. (2007): Recurrence of travelling waves in transitional pipe flow, *J. Fluid Mech.*, vol.584, pp. 69-102.

Kittelson, D. B. (1998): Engines and nanoparticles: A review, *J. Aerosol Sci.*, vol. 29, pp. 575-588.

Lee, K. W. (1983): Change of particle size distribution during Brownian coagulation. *J. Colloid Interf. Sci.*, vol. 92, pp. 315-325.

Lin, H.; Atluri, S. N. (2000): Meshless local Petrov-Galerkin (MLPG) method for convection-diffusion problems. *CMES: Computer Modeling in Engineering & Sciences*, vol. 1, pp. 45-60.

Lin, H.; Atluri, S. N. (2001): The meshless local Petrov-Galerkin (MLPG) method for solving incompressible Navier-Stokes equations. *CMES: Computer Modeling*

in Engineering & Sciences, vol. 2, pp. 117-142.

Lin, J. Z.; Chan, T. L.; Liu, S.; Zhou, K.; Zhou, Y.; Lee, S. C. (2007): Effects of coherent structures on nanoparticle coagulation and dispersion in a round jet. *Int. J. Nonlinear Sci. Numer. Simul.,* vol.8, pp. 45-54.

Liu, C.S.; Atluri, S. N. (2008): A novel time integration method for solving a large system of non-linear algebraic equations. *CMES: Computer Modeling in Engineering & Sciences*, vol. 31, pp. 71-83.

Liu, C.S.; Atluri, S. N. (2009): A highly accurate technique for interpolations using very high-order polynomials, and its applications to some ill-posed linear problems. *CMES: Computer Modeling in Engineering & Sciences*, vol. 43, pp. 253-276.

Lopez, J. M.; Shen, J. (1998): An efficient spectral projection method for the Navier-Stokes equations in cylindrical geometries I. Axisymmetric cases. *J. Comput Physics*, vol. 139, pp. 308-326.

Mellibovsky, F.; Meseguer, A. (2009): Critical threshold in pipe flow transition. *Philos. Trans. R. Soc. A- Math. Phys. Eng. Sci.*, vol. 367, pp. 545-560.

Meseguer, A.; Trefethen, L. N. (2003): Linearized pipe flow to Reynolds number 10^7. *J. Comput. Physics*, vol. 186, pp. 178-197.

Miller, S. E.; Garrick, S. C. (2004): Nanoparticle coagulation in a planar jet. *Aerosol Sci. Technol.*, vol. 38, 79-89.

Mohammadi, M. H. (2008): Stabilized Meshless Local Petrov-Galerkin (MLPG) Method for Incompressible Viscous Fluid Flows. *CMES: Computer Modeling in Engineering & Sciences*, vol. 29, pp. 75–94.

Orsini, P.; Power, H.; Morvan, H. (2008): Improving Volume Element Methods by Meshless Radial Basis Function Techniques. *CMES: Computer Modeling in Engineering & Sciences*, vol. 23, pp.187–208.

Otto, E.; Fissan, H.; Park, S. H. (1999): The log-normal size distribution theory of Brownian aerosol coagulation for the entire particle size range: Part II. Analytical solution using dahneke's coagulation kernel. *J. Aerosol Sci.,* vol. 30, pp. 17-34.

Pohjola, M.; Pirjola, L.; Kukkonen, J. ; Kulmala, M. (2003): Modelling of the influence of aerosol processes for the dispersion of vehicular exhaust plumes in street environment. *Atmos. Environ.,* vol. 37, pp. 339-351.

Pohjola, M.; Pirjola, L.; Kukkonen, J. ; Kulmala, M. (2006): Correction to modelling of the influence of aerosol processes for the dispersion of vehicular exhaust plumes in street environment. *Atmos. Environ.,* vol. 40, pp. 311-314.

Pope, C. A.; Dockery D. W. (2006): Health effects of fine particulate air pollution:

Lines that connect. *J. Air Waste Manage. Assoc.*, vol. 56, pp. 709-742.

Prakash, A.; Bapat, A. P.; Zachariah, M. R. (2003): A simple numerical algorithm and software for solution of nucleation, surface growth, and coagulation problems. *Aerosol Sci. Technol.,* vol. 37, pp. 892-898.

Pringle, C.C.T.; Kerswell, R. R. (2007): Asymmetric, helical and mirror-symmetric travelling waves in pipe flow. *Phys. Rev. Lett.*, vol. 99, 074502.

Pratsinis, S. E. (1988): Simultaneous nucleation, condensation, and coagulation in aerosol reactor. *J. Colloid Interf. Sci.*, vol. 124, pp. 416-427.

Pratsinis, S. E.; Kim, K. S. (1989): Particle coagulation, diffusion and thermophoresis in laminar tube flows. *J. Aerosol Sci.*, vol. 20, pp. 101-111.

Schneider, T. M.; Eckhardt, B.; Yorke, J. A. (2007): Turbulence transition and the edge of chaos in pipe flow. *Phys. Rev. Lett.*, vol. 99, 034502.

Sellountos, E. J.; Sequeira, A. (2008): A hybrid multi-region BEM/LBIE RBF velocity-vorticity scheme for the two-dimensional Navier-Stokes equations. *CMES: Computer Modeling in Engineering & Sciences*, vol. 23, pp. 127–148.

Sellountos, E. J.; Sequeira, A.; Polyzos, D. (2009): Elastic transient analysis with MLPG (LBIE) method and local RBFs. *CMES: Computer Modeling in Engineering & Sciences*, vol. 41, pp. 215-242.

Settumba, N.; Garrick, S. C. (2003): Direct numerical simulation of nanoparticle coagulation in a temporal mixing layer via a moment method. *J. Aerosol Sci.*, vol. 34, pp. 149-167.

Stone, V.; Donaldson, K. (1998): Small particles-big problem. The Aerosol Society Newsletter, vol. 33, pp. 12-14.

Sioutas, C., Delfino, R.J.; Singh, M. (2005): Review on exposure assessment for atmospheric ultrafine particles (UFPs) and implications in epidemiologic research. *Environ. Health Perspect.*, vol. 113, pp. 947-955.

Trefethen, L. N.; Trefethen, A. E.; Reddy, S.C.; Driscoll, T. A. (1993): Hydrodynamic stability without eigenvalues. *Science*, vol. 261, pp. 578-584

Upadhyay, R. R.; Ezekoye, O. A. (2003): Evaluation of the 1-point quadrature approximation in QMOM for combined aerosol growth laws. *J. Aerosol Sci.,* vol. 34, pp. 1665-1683.

van Doorne, C. W.; Westerweel J. (2009): The flow structure of a puff. *Philos. Trans. R. Soc. A- Math. Phys. Eng. Sci.*, vol. 367, pp. 489-507.

Xie, M. L.; Lin, J. Z.; Xing, F. T. (2007): On the hydrodynamic stability of a particle laden flow in growing flat plate boundary layer, *J. Zhejiang University-Sciences A, vol.* 8, pp. 275-284.

Xie, M. L.; Chan, T. L.; Zhang Y. D.; Zhou, H. C. (2008): Numerical analysis of nonlinear stability of two-phase flow in the Blasius boundary layer. *Int. J. Nonlinear Sci. Numer. Simul.,* vol. 9, pp. 423-434

Xie, M. L.; Lin, J. Z.; Zhou H. C. (2009a): Temporal stability of a particle-laden Blasius boundary layer. *Mod. Phys. Lett. B*, vol. 23, pp. 203-216.

Xie, M. L.; Lin, J. Z.; Zhou, H. C. (2009b): The effect of non-linear interaction between gas and particle velocities on the hydrodynamic stability in the Blasius boundary layer. *Int. J. Non-linear Mech*., vol. 44, pp. 106-114.

Xie, M. L.; Zhou H. C.; Zhang Y. D. (2009c): Hydrodynamics stability of Bickley jet with particle laden flow. *J. Hydrodynamics*, Ser. B, vol. 21, pp. 608-613.

Xie, M. L.; Zhou, H. C.; Chan, T. L. (2009d): An improved Petrov-Galerkin spectral collocation solution for linear stability of circular jet. *CMES: Computer Modeling in Engineering & Sciences*, vol. 46, pp. 271-289.

Xie, M. L.; Lin J. Z. (2009e): An efficient numerical solution for linear stability of circular jet: A combination of Petrov-Galerkin spectral method and exponential coordinate transformation based on Fornberg's treatment. *Int. J. Numer. Meth. Fluids*, vol. 61, pp. 780-795.

Yu, M. Z.; Lin, J. Z.; Chan, T. L. (2008a): A new moment method for solving the coagulation equation for particles in Brownian motion. *Aerosol Sci. Technol.*, vol. 42: 705-713

Yu, M. Z.; Lin, J. Z.; Chan, T. (2008b): Numerical simulation of nanoparticle synthesis in diffusion flame reactor. *Powder Tech.*, vol. 181, pp. 9-20.

Yu, M. Z.; Lin, J. Z.; Chan, T. L. (2008c): Effect of precursor loading on non-spherical TiO_2 nanoparticle synthesis in a diffusion flame reactor. *Chem. Eng. Sci*., vol. 63, pp. 2317-2329.